Heralding Multiple Photonic Pulsed Bell Pairs via Frequency-Resolved Entanglement Swapping

Sofiane Merkouche,[1,*] Valérian Thiel,[1] Alex O. C. Davis,[2] and Brian J. Smith[1]
[1]Department of Physics and Oregon Center for Optical, Molecular, and Quantum Science, University of Oregon, Eugene, Oregon 97403, USA
[2]Centre for Photonics and Photonic Materials, Department of Physics, University of Bath, Bath BA2 7AY, United Kingdom

(Received 24 May 2021; accepted 14 January 2022; published 11 February 2022)

Entanglement is a unique property of quantum systems and an essential resource for many quantum technologies. The ability to transfer or swap entanglement between systems is an important protocol in quantum information science. Entanglement swapping between photons forms the basis of distributed quantum networks. Here an experiment demonstrating entanglement swapping from two independent multimode time-frequency entangled sources is presented, resulting in multiple heralded frequency-mode Bell states. Entanglement in the heralded states is verified by measuring conditional anticorrelated joint spectra and quantum beating in two-photon interference. Our experiment heralds up to five orthogonal Bell pairs within the same setup, and this number is ultimately limited only by the entanglement of the initial sources.

DOI: 10.1103/PhysRevLett.128.063602

Entanglement, the correlations displayed between subsystems of a multipartite quantum system, is one of the most distinguishing properties of quantum physics and a significant resource for quantum information science and technology (QIST). Entanglement swapping [1] is a protocol that enables entanglement of quantum systems that have never interacted. These systems can be separated by large distances [2] or even exist at different times [3,4]. This protocol underpins efforts to realize large-scale quantum networks as the core element of quantum repeaters [5]. Furthermore, entanglement swapping can be used to probe the fundamental nature and extent of nonlocality of multipartite quantum systems [6].

For two-photon entanglement, Bell-state measurements, projecting onto two-mode entangled states, can be readily implemented using a beam splitter followed by mode-resolved measurements with 50% success probability. Entanglement swapping using the latter approach has been experimentally demonstrated using photons entangled in their polarization [7], spatial [8], and temporal [9] degrees of freedom. Recent work has shown that temporal- or pulse-mode encoding offers unique opportunities for QIS [10], and entanglement swapping of identical pulse-mode Bell states from engineered sources has recently been demonstrated [11]. Thus addressing pulse-mode entanglement manipulation and verification is a timely topic.

In this Letter, we report an experiment demonstrating pulsed frequency-mode entanglement swapping between two independent multimode entangled photon pair sources. This is enabled by the use of spectrally resolved detection [12] to implement projective measurements onto multiple frequency-encoded Bell states. The entanglement of the heralded two-photon states is verified by measurement of two-photon quantum beats [13], showing phase coherence between frequency components, and the joint-spectral intensity arising from fourfold frequency resolved measurements showing direct frequency anticorrelations. In this way we generalize the pulse-mode entanglement swapping scheme [11] to make full use of the inherent high-dimensional time-frequency entanglement available in off-the-shelf spontaneous parametric down conversion (SPDC) sources. To the best of our knowledge, this is the first experiment to demonstrate both heralding and discrimination of multiple Bell pairs with a single source and measurement apparatus, as well as the first experiment to perform frequency-resolved measurements of four photons.

The experimental setup for producing heralded frequency-mode-entangled two-photon states is shown schematically in Fig. 1. Here two SPDC sources of spectrally entangled photon pairs [14], labeled S1 and S2, are realized by pumping a nonlinear crystal, $\chi^{(2)}$, in a double pass configuration. The pump consists of frequency-doubled pulses derived from a Ti:sapphire (Ti:sapph) laser oscillator centered at 415 nm with 2.3 nm full width at half-maximum (FWHM) bandwidth with an 80 MHz repetition rate, and the SPDC is produced by collinear type-II phasematching within a 2.5 mm long bismuth triborate (BiBO) crystal. The double-pass configuration ensures that the two sources are identical. Signal and idler photons from both sources are collected into polarization-maintaining (PM) single-mode fibers. We measure a pair detection rate of up to 300 kHz from each source using superconducting nanowire single-photon detectors (SNSPDs).

 © 2022 American Physical Society

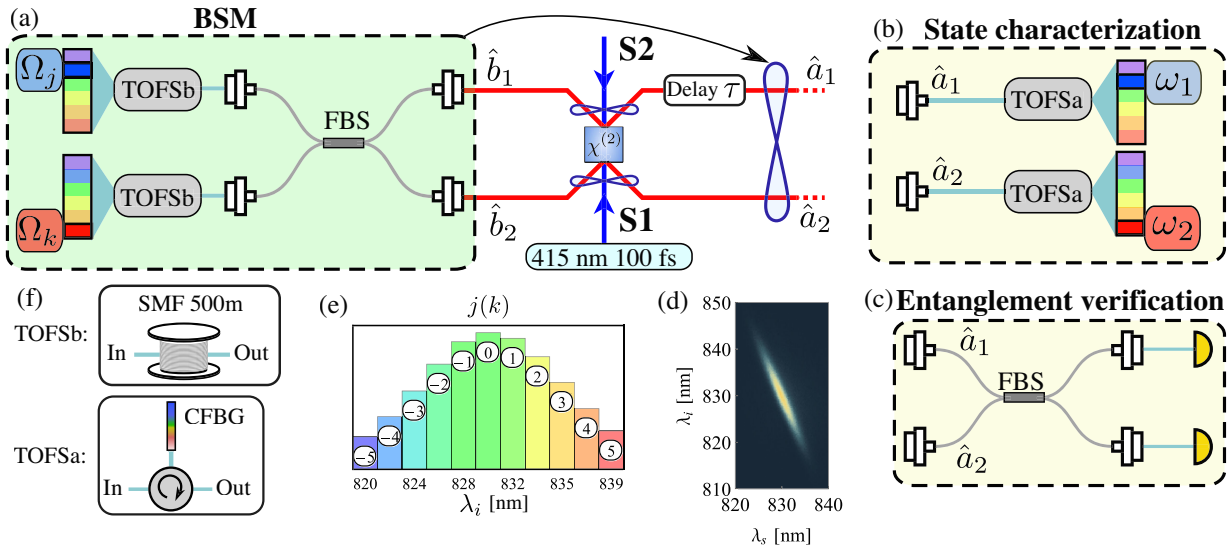

FIG. 1. Experimental setup (see main text for description): A single nonlinear crystal ($\chi^{(2)}$) is double-passed by a blue pump laser beam, effectively creating two SPDC sources (S1 and S2) of time-frequency entangled photon pairs. Clockwise: (a) The frequency-multiplexed Bell-state measurement (BSM) implemented on the idler photons in modes $\hat{b}_1$ and $\hat{b}_2$. FBS: fiber beam splitter. TOFSb: time-of-flight spectrometer for the idler photons. (b) State characterization: joint spectral measurement of the signal photons in modes $\hat{a}_1$ and $\hat{a}_2$, conditioned on the BSM. TOFSa: time-of-flight spectrometer for the signal photons. (c) Entanglement verification: two-photon interference as a function of relative delay τ, conditioned on the BSM. (d) Measured JSI for each of the sources, where $\lambda_s(\lambda_i)$ is the signal (idler) wavelength. (e) Spectrum of the idler photons as measured by TOFSb, showing the labeling convention for $\Omega_{j(k)}$ measurements, (e.g., Ω_0 corresponds to a bin centered at 830 nm). (f) Physical implementation of the dispersive time-of-flight spectrometers: TOFSb is a 500 m long single-mode fiber (SMF), and TOFSa is a highly dispersive chirped fiber Bragg grating (CFBG).

Signal ($\hat{a}$) and idler ($\hat{b}$) photons are generated for source 1(2) by pump pulses traveling from bottom to top (top to bottom). The signal and idler photons from each source display spectral-temporal correlations, as reflected by the joint spectral intensity measurement in Fig. 1(d). The four-photon state produced by this system when a pair of photons is generated in each source is given by

$$|\psi\rangle = \int d\omega_s d\omega_i d\omega_s' d\omega_i' f(\omega_s,\omega_i)\hat{a}_1^\dagger(\omega_s)\hat{b}_1^\dagger(\omega_i) \times f(\omega_s',\omega_i')\hat{a}_2^\dagger(\omega_s')\hat{b}_2^\dagger(\omega_i')|\mathrm{vac}\rangle. \quad (1)$$

Here $\hat{a}_{1(2)}^\dagger(\omega)(\hat{b}_{1(2)}^\dagger(\omega))$ creates a photon with frequency ω in the signal (idler) mode and 1(2) label source 1(2). The function $f(\omega_s,\omega_i)$ is the normalized complex joint spectral amplitude (JSA) of the two sources, assumed to be identical for both. The joint spectral intensity (JSI) $|f(\omega_s,\omega_i)|^2$ of each source is measured efficiently using a time-of-flight spectrometer consisting of a pair of 500 m-long fibers (TOFSb), as depicted in Fig. 1(f). Each photon from the signal-idler pair is passed through the dispersive fiber, imparting a wavelength-dependent delay. Time-resolved coincidence detection at the output, using a time-to-digital converter (ID900) with approximately 30 ps timing resolution, provides a measurement of the JSI with 0.5 nm resolution [see Fig. 1(d)]. Assuming negligible phase correlations [15], we estimate the amount of entanglement in each source by taking the square root of the JSI and calculating the Schmidt number [16], which yields a value $K \sim 4$.

To herald a frequency-mode entangled state of the signal photons in paths $\hat{a}_1$ and $\hat{a}_2$, a partial Bell-state measurement (BSM) on the idler photons in paths $\hat{b}_1$ and $\hat{b}_2$, is performed, as shown in Fig. 1(a). This is achieved by interfering the fields at a balanced PM fiber beam splitter (FBS) and making frequency-resolved coincident measurements at the output. A coincidence detection centered on frequencies Ω_j and Ω_k projects the input idler fields onto the two-color singlet Bell state $|\psi^-\rangle = (1/\sqrt{2})\times(|\Omega_j\rangle_{b1}|\Omega_k\rangle_{b2} - |\Omega_k\rangle_{b1}|\Omega_j\rangle_{b2})$, where $|\Omega_j\rangle_{b1(2)}$ is a single-photon state occupying a narrow-band spectral mode centered on frequency Ω_j. Here j and k are integers labeling different "frequency-bin" measurement outcomes in the spectrometers, of which there are approximately 15. Care must be taken to ensure the idler photons from sources 1 and 2 arrive at the FBS simultaneously, which is achieved using a free-space delay line in path $\hat{b}_1$ (not shown). By scanning the delay line and monitoring coincidences between the two outputs of the FBS one can observe a Hong-Ou-Mandel dip between the idler photons [13]. Upon a coincidence detection of the idler photons in frequency bins j and k at the output of TOFSb, the state heralded in the signal fields is well approximated by [17]

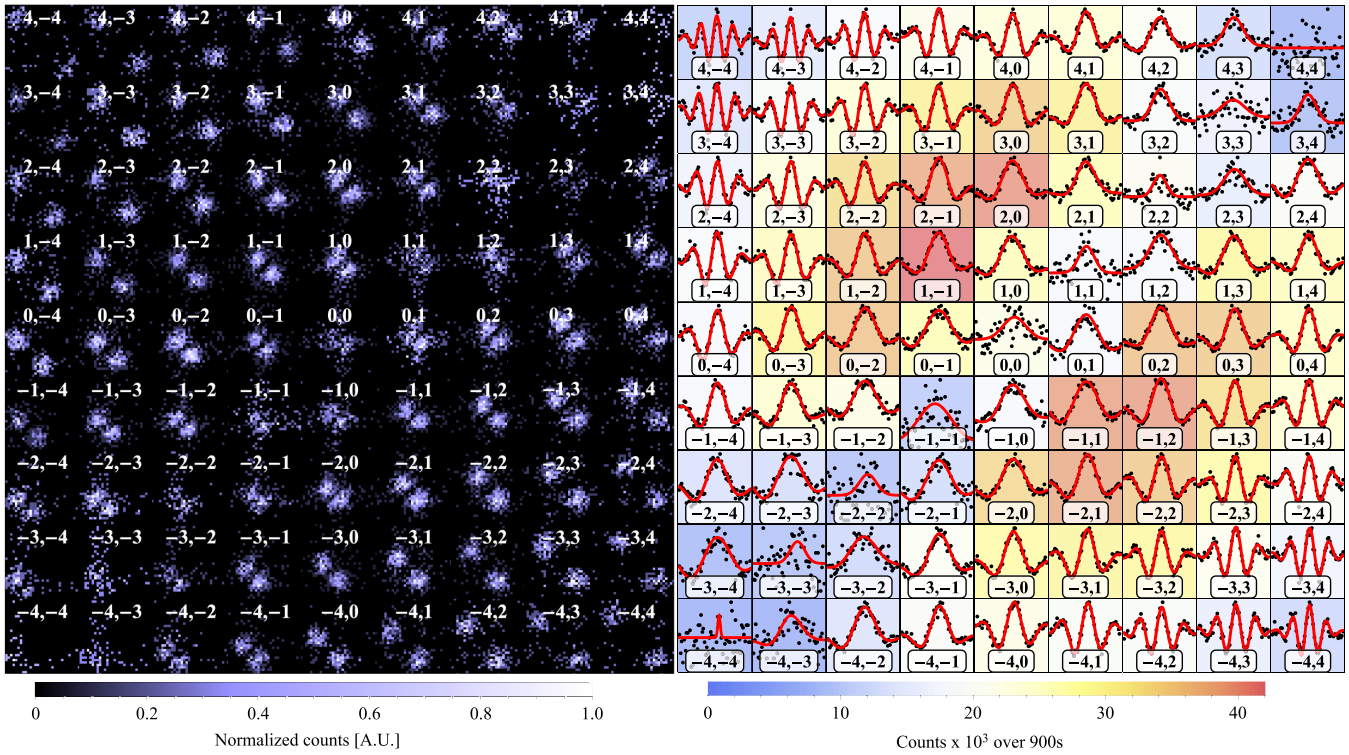

FIG. 2. Left, state characterization: array of the measured JSIs F_{jk} of the signal photons, conditioned on the (Ω_j, Ω_k) outcomes of the BSM. Right, entanglement verification: array of interference fringes $P_{jk}(\tau)$, conditioned on the same (Ω_j, Ω_k) outcomes, verifying entanglement of the states. The background color indicates the total number of counts for each plot, and thus the entire array maps out the p_{jk} matrix. Each array was obtained in a single measurement run. For the axes of each plot, see Fig. 3 (right).

$$|\Psi_{jk}\rangle = \frac{1}{\sqrt{2\mathcal{C}_{jk}}}(|\phi_j\rangle_1|\phi_k\rangle_2 - |\phi_k\rangle_1|\phi_j\rangle_2). \tag{2}$$

Here the signal photons occupy spectral modes $\phi_j(\omega) \propto f(\omega, \Omega_j)$ that depend on the heralding frequency bin j and the source JSA. The labeling of these bins is done according to an experimental calibration as shown in Fig. 1(e). We approximate the spectral amplitudes by a Gaussian $\phi_j(\omega) \propto \exp[-(\omega - \omega_j)^2/4\sigma^2]$, with ω_j and σ determined by the JSA and heralding frequency bin. The normalization coefficient is $\mathcal{C}_{jk} = 1 - |\langle\phi_j|\phi_k\rangle|^2$, which depends on the spectral mode overlap [17]. Note that since the TOFSs have multiple measurement outcomes, we can herald several different entangled two-photon states $|\Psi_{jk}\rangle$ in a single experimental configuration. In Fig. 5 of Ref. [17], we show graphically how a detection of an idler photon at Ω_j projects its corresponding signal photon onto a state with spectral distribution $|\phi_j(\omega)|^2$.

The heralded states in Eq. (2) can be characterized by measuring the JSI, $F_{jk}(\omega_1, \omega_2) \propto |\phi_j(\omega_1)\phi_k(\omega_2) - \phi_k(\omega_1)\phi_j(\omega_2)|^2$, using another, higher-resolution, method of frequency-to-time mapping (TOFSa), as indicated in Fig. 1(b). These TOFSa are constructed using a chirped fiber Bragg grating (CFBG), shown in Fig. 1(c), instead of fibers, for greater dispersion that provides increased spectral resolution of 0.1 nm [12]. Figure 2, left, shows the measured JSI for 81 different heralding outcomes j, k, where the heralding measurement outcomes j, k are integers between −4 and 4, labeled by binning the data according to Fig. 1(e). These demonstrate that the heralded two-photon states do indeed have spectral amplitude anticorrelations. However, this measurement alone is not sufficient to demonstrate entanglement, beyond classical correlations.

To verify entanglement in the state $|\Psi_{jk}\rangle$, beyond frequency anticorrelations, two-photon interference is used in a manner similar to the method employed in Ref. [11]. Here the heralded signal photons are detected in coincidence at the output of a balanced FBS, as a function of relative arrival time delay τ, as depicted in Fig. 1(c). If the photons are not entangled one predicts a Hong-Ou-Mandel (HOM) dip in the coincidence events at zero delay. However, if the photons occupy an antisymmetric entangled state there is a HOM peak at zero delay [18]. For the heralded state $|\Psi_{jk}\rangle$, the coincidence probability as a function of the delay between the signal photons arriving at the FBS is [17]

$$P_{jk}(\tau) = 1/2 + e^{-\tau^2\sigma^2}\cos[(\omega_j - \omega_k)\tau]/2, \tag{3}$$

which oscillates at the difference frequency $\omega_j - \omega_k$. These oscillations, obtained without filtering of the interfering

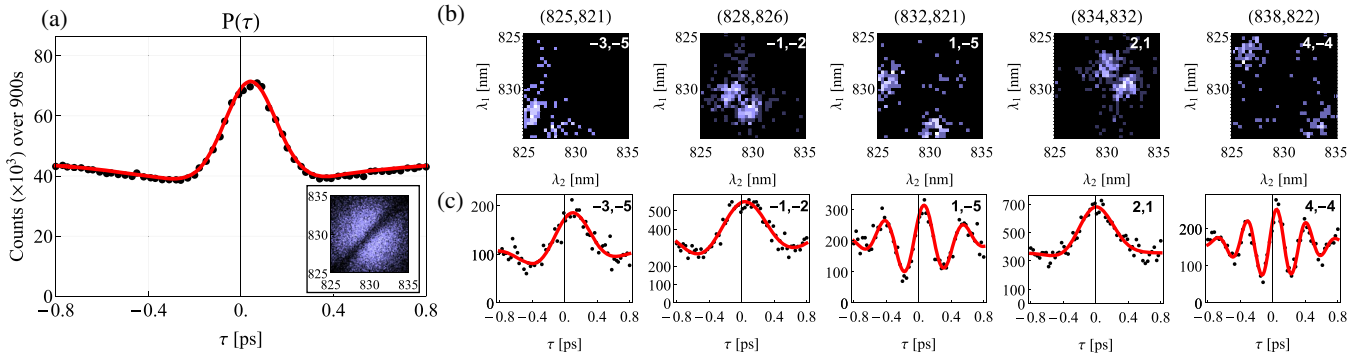

FIG. 3. (a) The integrated interference fringes $P(\tau)$. The red plot is not a fit, but the sum of the fits from Fig. 2(b). The inset is the integrated JSI $F(\omega_1, \omega_2)$. (b) A set of JSIs and interference fringes (c) corresponding to five quasiorthogonal modes, satisfying an overlap of ≤ 0.15 as described in the text, chosen from the full set from Fig. 2.

fields, are a hallmark of two-color entanglement of the input state [18]. The heralded two-photon interference coincidence rate as a function of delay τ between signal photons is shown in Fig. 2, right. Indeed, if the photons had only spectral anticorrelations, but no well-defined spectral phase relationship, the coincidence rate would be independent of the time delay τ. Note that for SPDC sources the probability that one source produces two pairs of photons is on the same order as the probability that each source produces a single pair. This contributes to additional terms in the heralded state inherent to all similar entanglement swapping experiments using SPDC [19]. This results in a constant coincidence background in the HOM measurement that is determined by blocking each signal path and recording coincidence events at the output of the beam splitter. After this background is subtracted, the measured visibility of the interference fringes is over 75%, consistent with the maximum visibility expected from source matching measurements [17]. Finally, it is notable that the total number of fourfold coincidence events for each (j, k) is proportional to the probability p_{jk} of heralding the state $|\Psi_{jk}\rangle$. We highlight this fact by coloring the background of the interference plots according to the total number of counts. The color map shown in Fig. 2, right, therefore represents the joint-spectral distribution for the idler photons measured after the beam splitter, where the trough along the diagonal $(j = k)$ is due to Hong-Ou-Mandel interference.

If the heralding measurements performed on the idler photons are not spectrally resolved, then the signal photons are heralded in a mixed state, $\hat{\rho} = \sum_{j,k} p_{jk} |\Psi_{jk}\rangle\langle\Psi_{jk}|$, which can be normalized by dividing by $\sum_{jk} p_{jk}$. The JSI for this state is just a weighted sum of the spectrally resolved heralded JSIs, $F_{jk}(\omega_1, \omega_2)$, given by $F(\omega_1, \omega_2) = \sum_{j,k} p_{jk} F_{jk}(\omega_1, \omega_2)$.

The heralded mixed state $\hat{\rho}$ retains the antisymmetry of its constituent states $|\Psi_{jk}\rangle$. This is evidenced by the two-photon interference pattern given by $P(\tau) = \sum_{j,k} p_{jk} P_{jk}(\tau)$, which predicts that the coincidence peak remains at $\tau = 0$. Two notable features arise from the inherent antisymmetry of the state. First, there is no amplitude in the JSI of the heralded mixed state along the diagonal $\omega_j = \omega_k$, as displayed in the inset of Fig. 3(a). Second, the antisymmetry of the state leads to a HOM-like peak in the two-photon interference $P(\tau)$, which is displayed in Fig. 3(a). Note also that the red curve in that plot is not a new fit to the data, but rather just the weighted sum of the individual fits to the $P_{jk}(\tau)$. Remarkably, the approximation that a spectrally resolved herald projects the signal onto a pure state is shown to be valid, and leads to the standard result of quantum mechanics that any mixed state may be represented as a convex combination of pure states. Taken all together, our data nicely highlights the quantum nature of measurement, whereby different quantum states arise as a consequence of different measurement results.

In the present experiment, the number of states $|\Psi_{jk}\rangle$ that we can herald is limited by the spectral resolution of the heralding spectrometers and the bandwidth of the idler photons. However, not all these states are orthogonal. This is due to the finite number of available orthogonal modes produced by the initial SPDC sources, quantified by the Schmidt number. A combinatorics argument shows that, for two identical sources with Schmidt number K, one can herald at most $K(K-1)/2$ orthogonal Bell pairs [8]. The ideal Bell state measurement for our scheme would resolve the idlers in the Schmidt mode basis of the sources, which could be accomplished by using a quantum pulse gate for instance [20], thus automatically heralding the signals in orthogonal Bell pairs. Since we perform spectrally resolved measurement of the idler photons into frequency bins, we herald more signal states than those comprising an orthogonal set. We can then simply choose a quasiorthogonal set of states from our data which satisfy an overlap criterion of $\int d\omega_1 d\omega_2 F_{jk}(\omega_1, \omega_2) F_{j'k'}(\omega_1, \omega_2) \leq \epsilon, \ \forall\, (j, k) \neq (j', k')$, where ϵ can be chosen arbitrarily small. In an application setting such as multiplexed entanglement distribution, one could in principle restrict consideration to this smaller set of

j, k heralding events which correspond to orthogonal states to avoid any unwanted crosstalk between frequency channels. In Fig. 3(b), we show a representative set of quasiorthogonal modes selected with $\epsilon = 0.15$, along with the associated interference fringes in Fig. 3(c). In this case there are five orthogonal modes, while our estimated K of 4 predicts a maximum of six orthogonal modes.

In conclusion, we have demonstrated a multimode frequency entanglement swapping scheme that is easily implemented with SPDC sources based upon dispersive, time-of-flight spectral measurements. Our design provides a simple way of heralding a high number of orthogonal frequency Bell pairs that is completely measurement based and is compatible with a variety of frequency-entangled sources. The ability to scale this approach to a larger number of orthogonal states is straightforward, requiring only entangled photon pair sources with a higher Schmidt number. We note that, in a manner similar to recent approaches to heralding single photons in pure quantum states [21,22], our protocol could be combined with frequency translators in the signal beams [23], to generate multiple copies of the same Bell state using a variety of broadband sources. A further extension of our work to entanglement swapping of higher-dimensional (HD) states through implementation of HD Bell state measurements, as recently demonstrated for path [24,25] and orbital-angular momentum [26], could be readily implemented using ancilla photons and an additional multiport beam splitter. Alternatively, the nonlinear optical process of sum-frequency generation has been proposed as a means to implement projective measurements onto HD entangled two-photon states [27]. Finally, with the advent of push-button sources of entangled photon pairs [28], multiplexed quantum repeaters of the kind that our protocol allows could prove to be a scalable solution for quantum communication networks, for instance, by serving as nodes in a network where the communicating parties are assigned different frequency channels.

This project has received funding from the European Union's Horizon 2020 research and innovation program under Grant Agreement No. 665148, the United Kingdom Defense Science and Technology Laboratory (DSTL) under Contract No. DSTLX-100092545, and the National Science Foundation under Grant No. 1839216.

S. M. and V. T. contributed equally to this work.

*Corresponding author.
oqt@uoregon.edu

[1] M. Źukowski, A. Zeilinger, M. A. Horne, and A. K. Ekert, Phys. Rev. Lett. **71**, 4287 (1993).
[2] H. de Riedmatten, I. Marcikic, J. A. W. van Houwelingen, W. Tittel, H. Zbinden, and N. Gisin, Phys. Rev. A **71**, 050302(R) (2005).
[3] A. Peres, J. Mod. Opt. **47**, 139 (2000).
[4] X.-s. Ma, S. Zotter, J. Kofler, R. Ursin, T. Jennewein, Č. Brukner, and A. Zeilinger, Nat. Phys. **8**, 479 (2012).
[5] H.-J. Briegel, W. Dür, J. I. Cirac, and P. Zoller, Phys. Rev. Lett. **81**, 5932 (1998).
[6] C. Branciard, D. Rosset, N. Gisin, and S. Pironio, Phys. Rev. A **85**, 032119 (2012).
[7] J.-W. Pan, D. Bouwmeester, H. Weinfurter, and A. Zeilinger, Phys. Rev. Lett. **80**, 3891 (1998).
[8] Y. Zhang, M. Agnew, T. Roger, F. S. Roux, T. Konrad, D. Faccio, J. Leach, and A. Forbes, Nat. Commun. **8**, 632 (2017).
[9] M. Halder, A. Beveratos, N. Gisin, V. Scarani, C. Simon, and H. Zbinden, Nat. Phys. **3**, 692 (2007).
[10] B. Brecht, D. V. Reddy, C. Silberhorn, and M. G. Raymer, Phys. Rev. X **5**, 041017 (2015).
[11] F. Graffitti, P. Barrow, A. Pickston, A. M. Brańczyk, and A. Fedrizzi, Phys. Rev. Lett. **124**, 053603 (2020).
[12] A. O. C. Davis, P. M. Saulnier, M. Karpiński, and B. J. Smith, Opt. Express **25**, 12804 (2017).
[13] Z. Y. Ou and L. Mandel, Phys. Rev. Lett. **61**, 54 (1988).
[14] A spectrally entangled two-photon state of light is one that can be written, in general, as $|\Psi\rangle = \int d\omega d\omega' f(\omega,\omega')\hat{a}^\dagger(\omega)\hat{b}^\dagger(\omega')|\text{vac}\rangle$, where $f(\omega,\omega')$ is not factorable into a product of the form $g(\omega)h(\omega')$.
[15] A. O. C. Davis, V. Thiel, and B. J. Smith, Optica **7**, 1317 (2020).
[16] C. K. Law, I. A. Walmsley, and J. H. Eberly, Phys. Rev. Lett. **84**, 5304 (2000).
[17] S. Merkouche, V. Thiel, and B. J. Smith, companion paper, Phys. Rev. A **105**, 023708 (2022).
[18] S. Ramelow, L. Ratschbacher, A. Fedrizzi, N. K. Langford, and A. Zeilinger, Phys. Rev. Lett. **103**, 253601 (2009).
[19] C. Wagenknecht, C.-M. Li, A. Reingruber, X.-H. Bao, A. Goebel, Y.-A. Chen, Q. Zhang, K. Chen, and J.-W. Pan, Nat. Photonics **4**, 549 (2010).
[20] D. V. Reddy and M. G. Raymer, Optica **5**, 423 (2018).
[21] M. Grimau Puigibert, G. H. Aguilar, Q. Zhou, F. Marsili, M. D. Shaw, V. B. Verma, S. W. Nam, D. Oblak, and W. Tittel, Phys. Rev. Lett. **119**, 083601 (2017).
[22] T. Hiemstra, T. F. Parker, P. Humphreys, J. Tiedau, M. Beck, M. Karpiński, B. J. Smith, A. Eckstein, W. S. Kolthammer, and I. A. Walmsley, Phys. Rev. Applied **14**, 014052 (2020).
[23] L. J. Wright, M. Karpiński, C. Söller, and B. J. Smith, Phys. Rev. Lett. **118**, 023601 (2017).
[24] Y.-H. Luo, H.-S. Zhong, M. Erhard, X.-L. Wang, L.-C. Peng, M. Krenn, X. Jiang, L. Li, N.-L. Liu, C.-Y. Lu, A. Zeilinger, and J.-W. Pan, Phys. Rev. Lett. **123**, 070505 (2019).
[25] X.-M. Hu, C. Zhang, B.-H. Liu, Y. Cai, X.-J. Ye, Y. Guo, W.-B. Xing, C.-X. Huang, Y.-F. Huang, C.-F. Li, and G.-C. Guo, Phys. Rev. Lett. **125**, 230501 (2020).
[26] M. Erhard, M. Malik, M. Krenn, and A. Zeilinger, Nat. Photonics **12**, 759 (2018).
[27] S. Merkouche, V. Thiel, and B. J. Smith, Phys. Rev. A **103**, 043711 (2021).
[28] L. Ginés, C. Pepe, J. Gonzales, N. Gregersen, S. Höfling, C. Schneider, and A. Predojević, Opt. Express **29**, 4174 (2021).